

AD-A102 633

PENNSYLVANIA STATE UNIV UNIVERSITY PARK IONOSPHERE R--ETC F/G 4/1
INFORMATION CONTENT ANALYSIS FOR THE PENN STATE UPPER ATMOSPHER--ETC(U)

JAN 81 J TSOU

N00014-79-C-0610

UNCLASSIFIED

PSU-IRL-SCI-468

NL

1 OF 1
AD A
102633

END
DATE
FILMED
9-81
DTIC

AD A102633

REF ID: A102633

LEVEL

DTIC
ELECTE
AUG 1 0 1981
C

12

DISTRIBUTION STATEMENT
Approved for public release
Distribution is unlimited

SECURITY CLASSIFICATION OF THIS PAGE (When Data Entered)

REPORT DOCUMENTATION PAGE		READ INSTRUCTIONS BEFORE COMPLETING FORM
1. REPORT NUMBER (14) PSU-IRL-SCI-468	2. GOVT ACCESSION NO. A702633	3. RECIPIENT'S CATALOG NUMBER
4. TITLE (and Subtitle) (6) Information Content Analysis for the Penn State Upper Atmospheric Water Vapor-Microwave Radiometer Experiment	5. TYPE OF REPORT & PERIOD COVERED (9) Technical Report	
7. AUTHOR(s) (10) Jung-Jung/Tsou	6. PERFORMING ORG. REPORT NUMBER PSU-IRL-SCI-468	
	(15) 8. CONTRACT OR GRANT NUMBER(s) N00014-79-C-0610	
9. PERFORMING ORGANIZATION NAME AND ADDRESS The Pennsylvania State University 318 Electrical Engineering East University Park, PA 16802	10. PROGRAM ELEMENT, PROJECT, TASK AREA & WORK UNIT NUMBERS Task No. NR 089-148	
11. CONTROLLING OFFICE NAME AND ADDRESS Office of Naval Research Code 464 Arlington, Virginia 22217	(11) 12. REPORT DATE January, 1981 (12) 31	
	13. NUMBER OF PAGES 20	
14. MONITORING AGENCY NAME & ADDRESS (if different from Controlling Office)	15. SECURITY CLASS. (of this report) Unclassified	
	15a. DECLASSIFICATION/DOWNGRADING SCHEDULE	
16. DISTRIBUTION STATEMENT (of this Report) Distribution Unlimited		
17. DISTRIBUTION STATEMENT (of the abstract entered in Block 20, if different from Report)		
18. SUPPLEMENTARY NOTES C		
19. KEY WORDS (Continue on reverse side if necessary and identify by block number) Structure of the Upper Atmosphere Ground-Based Techniques and Measurements Data Analysis Techniques		
20. ABSTRACT (Continue on reverse side if necessary and identify by block number) A ground based, microwave radiometer system is being completed at IRL which will be used to measure mesospheric water vapor. The present study addresses itself to the basic radiative transfer of this experiment and to the interaction between the atmosphere and electromagnetic radiation. Using a classical mathematical analysis of the data inversion process an estimation of the true information content of the received data is produced. This process depends critically upon the structure of the weighting functions as was anticipated.		

DD FORM 1 JAN 73 1473

EDITION OF 1 NOV 65 IS OBSOLETE
S/N 0102-014-6601

SECURITY CLASSIFICATION OF THIS PAGE (When Data Entered)

788430
x16

SECURITY CLASSIFICATION OF THIS PAGE(When Data Entered)

The result of this study is that the present radiometer system should have four clearly independent pieces of information per profile, with a fifth piece possible, for realistic estimates of system errors.

Accession No.	
DTIC TAB	<input checked="checked" type="checkbox"/>
Unannounced	<input type="checkbox"/>
Justification	
By	
Distribution/	
Availability Codes	
Dist	Avail and/or Special
A	

NONE

SECURITY CLASSIFICATION OF THIS PAGE(When Data Entered)

PSU-IRL-SCI-468

Classification Numbers: 1.9, 3.2.1, 3.2.3

Scientific Report 468

Information Content Analysis for the
Penn State Upper Atmospheric Water Vapor-
Microwave Radiometer Experiment

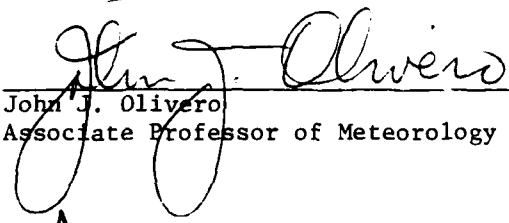
by

Jung-Jung Tsou

January, 1981

The research reported in this document has been supported by the
Office of Naval Research under Contract No. N00014-79-C-0610

Submitted by:


John J. Olivero
Associate Professor of Meteorology

Approved by:


John S. Nisbet
Director, Ionosphere Research Laboratory

Department of Electrical Engineering
Ionosphere Research Laboratory
The Pennsylvania State University
University Park, Pennsylvania 16802

Table of Contents

	Page
ABSTRACT	ii
LIST OF TABLES	iii
LIST OF FIGURES	iv
ACKNOWLEDGEMENTS	v
I INTRODUCTION	1
II RADIATIVE TRANSFER	2
III INFORMATION CONTENT	7
IV RESULTS AND DISCUSSION	13
V ZENITH ANGLE EFFECTS	15
VI SUMMARY AND CONCLUSION	16

Abstract

A ground based, microwave radiometer system is being completed at IRL which will be used to measure mesospheric water vapor. The present study addresses itself to the basic radiative transfer of this experiment and to the interaction between the atmosphere and electromagnetic radiation.

Using a classical mathematical analysis of the data inversion process an estimation of the true information content of the received data is produced. This process depends critically upon the structure of the weighting functions as was anticipated.

The result of this study is that the present radiometer system should have four clearly independent pieces of information per profile, with a fifth piece possible, for realistic estimates of system errors.

List of Tables

Table I (Eigenvalues λ and Corresponding Channel/Kernel Numbers k).

Table II (Channel/Kernel Frequency).

List of Figures

- Fig. 1: The 25 normalized kernels plotted against height, zero zenith angle, emission case.
- Fig. 2: The four independant (information containing) kernels plotted versus height (solid curves); a possible fifth, information containing, kernel (unconnected symbols).
- Fig. 3: The estimated number of independant kernels, dependant upon the number of measurement, for different possible error levels.

Acknowledgements

The author wishes to thank the Office of Naval Research for its support of this project under contract number N00014-79-C-0610.

1. Introduction

Information on the vertical profiles of each element existing in the atmosphere can provide a better understanding of the atmosphere. This is especially true for the water vapor content which plays a dominant role in photochemistry in the middle atmosphere (stratosphere and mesosphere). Therefore, investigating the concentration of water vapor in the atmosphere is very important.

There are two major ways to do the measurements: in-situ, and remote sensing techniques. The vertical profiles of H_2O in the lower atmosphere can be determined by balloon sounding. However, in the upper atmosphere where the H_2O content is much less compared with the H_2O in the troposphere, contamination may cause difficulties in determining the correct amount. Therefore, the remote sensing technique, which can allow us to study the atmospheric region without disturbing it, is a very attractive solution. Here we choose the microwave rather than the IR remote sensing technique to investigate the H_2O content in the upper atmosphere. The major reason is that the characteristic spectrum of H_2O has many more and closer spaced absorption lines in the IR region than in the microwave region, and the collisions among air molecules and gases will significantly broaden the absorption bands, thus the overlapping among the absorption bands decreases the vertical resolution. Besides, the microwave radiometer can detect at lower power level and penetrate through clouds which are opaque to IR.

According to kinetic theory (Goody, 1964), the lines of the characteristic spectrum of each molecule will be broadened both by collision effects between molecules and by Doppler broadening. The former, depending on the pressure of gas, dominates in the lower atmosphere and decreases exponentially with height, while the latter, depending upon random molecular motions hence temperature, contributes significantly only at

levels above 80 Km. The H_2O content in the atmosphere is found mostly within the troposphere having only a very small contribution at higher levels. The corresponding spectrum of this H_2O concentration should be much more smooth and broadened at lower levels, narrowing to a small amplitude but much sharper peak at upper levels. Such differences in the half-width of the spectral peak can allow a microwave radiometer to be set up at ground level and measure the radiation being absorbed or emitted from H_2O throughout the atmosphere.

2. Radiative Transfer

Water vapor has only two characteristic lines existing in the microwave region -- 22 GHz, 183 GHz. The 183 GHz line is much more intense but its attenuation through the troposphere is so strong that it can only be used from platforms aloft, such as by satellite through a limb viewing measurement. For a ground-base microwave measurement of H_2O , one must use the rotational line centered at 22 GHz. The vertical resolution is determined by the spectral line width and the bandwidth of the radiometer, thus setting the lower height limit of H_2O content one can determine. (The radiometer in question is constructed with a filter bank centered at 22.235 GHz, covering a half width of 2.5 MHz, using 50 channels; the predicted measurable height range is 50 to 85 Km.)

The wavelengths of the microwave region range from 10 cm to 1 mm, which is in the Rayleigh-Jeans region of the Plank black-body function. This provides a simple relationship between the emission power of the medium and its thermal absolute temperature; that is, the emission power is proportional to the temperature and also to the concentration of the gas at that level. The opacity of the atmosphere to radiation is due to the absorption and scattering of air molecules (through their vibrational and rotational motions), and the interaction between air molecules and radiation

field may emit quantized energy. Since the scattering effects are much smaller than the other two, only the absorptions and emissions are considered here. Assuming local thermal equilibrium (LTE) in the atmosphere, the linear relationship between the measured intensity of the radiation and the atmospheric (thermal) temperature allows one to specify the radiative transfer in the following form, at frequency ν :

$$T_B(\nu) = T_S(\nu)e^{-\tau(\nu)} + \int_h^\infty T(\nu,s) \cdot K(\nu,s) \cdot e^{-\tau(\nu)} ds \quad (1)$$

$T_B(\nu)$ = the brightness temperature

$T_S(\nu)$ = the thermal temperature of an external source

$T(\nu,s)$ = the kinetic temperature of atmosphere

$K(\nu,s)$ = the total absorption coefficient

ds = the optical path length

and $\tau(\nu) = \int_h^\infty K(\nu,s) \cdot ds$ = the optical depth (or opacity).

On the right hand side of eq.(1), the first term is the transmission of external radiation S and the second term involves the emission of the medium.

In order to simplify the nonlinearity between the absorption coefficient and the optical path, some approximations can be made. Consider the atmosphere to be a series of homogeneous, 1 Km thick layers, and take the average value of temperature and pressure in each layer to estimate the cross section of the constituent (σ). The refraction effects in the atmosphere which have been calculated are too small to be included (Longbothum, 1976). In this case, the effective emission of the medium (in the radiative transfer equation which involves the integration over the range of interest) can be written as the sum of the contributions from each layer attenuated through all the layers below. That is:

$$\int_h^\infty T(\nu, s) \cdot K(\nu, s) e^{-\tau(\nu)} ds \approx \sum_{i=1}^N \bar{T}_i(\nu) \cdot \exp \left[-\sum_{j=1}^{i-1} \tau(\nu, s_j) \right] \cdot \left(1 - e^{-\tau(\nu, s_i)} \right) \quad (2)$$

and thus where \bar{T}_i is the average temperature in the layer i , and

$$\tau(\nu) = \sum_{i=1}^N \tau(\nu, s_i) \approx \sum_{i=1}^N \int_{s(\nu, h_i)}^{s(\nu, h_{i+1})} K(\nu, s) \cdot ds \approx \sum_{i=1}^N \frac{[K(\nu, s_{i+1}) + K(\nu, s_i)] \cdot \Delta s}{2} \quad (3)$$

where N is the number of layers.

Therefore, the total brightness temperature is:

$$T_B(\nu) = T_S(\nu) \exp \left[-\sum_{j=1}^N \tau(\nu, s_j) \right] + \sum_{i=1}^N \bar{T}_i(\nu) \exp \left[-\sum_{j=1}^{i-1} \tau(\nu, s_j) \right] \cdot \left(1 - e^{-\tau(\nu, s_i)} \right) \quad (4)$$

For an absorption experiment, the second term on the right hand side of the eq. (4) is negligible. In order to avoid the uncertainties in the solar temperature at the wavelengths of the microwave region, the method of calculating the ratio of brightness temperature at two different zenith angles is preferred. Operating the ground base radiometer at zenith angle (ϕ) lower than 80° , allows one to approximate the spherical earth geometry by a plane earth, i.e. ds can be written as $\sec \phi \cdot dz$; then we get:

$$\sum_{j=1}^N \tau(\nu, z_j) = \frac{\ln(T_{B1}/T_{B2})}{(\sec. \phi_2 - \sec. \phi_1)} \quad (5)$$

where we define:

$$\tau(\nu, z_j) = \int_{z_j(\nu)}^{z_{j+1}(\nu)} K(\nu, z) \cdot dz$$

and the superscript 1 and 2 stand for the cases at different zenith angles ϕ_1 , and ϕ_2 . The quantity of the right hand side of the eq. (5) can be determined directly through measurements, thus defined as $g(\nu)$ or g_i , where i stands for the different frequency dependence.

Generally, the absorption coefficient $K(\nu, s)$ for optical path s at frequency ν can be written as the product of the volumetric concentration of the constituent $n(s)$ and the total extinction cross section $\sigma(\nu, s)$. The weak dependence of $K(\nu, s)$ on $n(s)$ has been tested over a range which corresponds to volumetric mixing ratios of 1 to 18 ppm. $K(\nu, s)$ varies only from 0.992 to 0.995 Km^{-1} over this range, to the first approximation it is separable. Thus we apply the mean value for each layer and the optical path becomes

$$\tau(\nu, z_j) = \int_{z_j(\nu)}^{z_{j+1}(\nu)} K(\nu, z) dz = [\bar{n}(z_j) \cdot \frac{\sigma(\nu, z_j) + \sigma(\nu, z_{j+1})}{2}] \cdot \Delta z_j \quad (6)$$

$$= WF_i(z_j) \cdot \bar{n}(z_j)$$

where $WF_i(z_j)$ is defined as $\frac{\Delta z}{2} \cdot [\sigma(\nu, z_j) + \sigma(\nu, z_{j+1})]$ and is called the i th weighting function. Therefore the relation becomes.

$$g_i = \sum_{j=1}^N WF_i(z_j) \cdot \bar{n}(z_j) \quad (7)$$

Consider the emission experiment; the second term on the right-hand-side of eq. (1) must then dominate. This term can be approximated as:

$$T_B^{-1}(\nu) = \sum_{i=M+1}^N \bar{T}_i (1 - e^{-\tau(\nu, s_i)}) \cdot \exp \left\{ - \left[\sum_{j=1}^M \tau(\nu, s_j) + \sum_{j=M+1}^{i-1} \tau(\nu, s_j) \right] \right\} \quad (8)$$

where $T_B^{-1}(\nu)$ = the upper atmospheric contribution to the brightness temperature in which we are interested; thus equals the total brightness temperature, $T_B(\nu)$, minus the lower atmosphere contribution which can be thought of as a base line (and is assumed to encompass layer 1 to layer M). Since $\tau(\nu, s_i) \ll 1$ and $\sum_{j=1}^M \tau(\nu, s_j) \gg \sum_{j=M+1}^{i-1} \tau(\nu, s_j)$, the equation becomes:

$$\begin{aligned}
 T_B^{-1}(\nu) &= \sum_{i=M+1}^N \bar{T}_i \cdot \exp \left\{ - \sum_{j=1}^M \tau(\nu, s_j) \right\} \cdot \frac{\Delta s_i}{2} \cdot [\sigma(\nu, s_i) + \sigma(\nu, s_{i+1})] \cdot \bar{n}(s_i) \\
 &\equiv \sum_{i=M+1}^N WF(\nu, s_i) \cdot \bar{n}(s_i)
 \end{aligned} \tag{9}$$

And here $WF(\nu, s_i)$ for the emission case corresponds to

$$\sum_{i=M+1}^N \bar{T}_i \cdot \exp \left\{ - \sum_{j=1}^N \tau(\nu, s_j) \right\} \cdot \frac{\Delta s_i}{2} \cdot [\sigma(\nu, s_i) + \sigma(\nu, s_{i+1})].$$

It can also be written in a more general form as:

$$g_i = \sum_{j=M+1}^N WF_i(s_j) \cdot \bar{n}(s_j) \tag{10}$$

where i stands for the frequency dependence, and $s_j = z_i \cdot \sec \phi$. With an appropriate inversion method, the water vapor content ($\bar{n}(z_i)$) in either case can be determined.

3. Information Content

Generally, an indirect remote sensing measurement has the following form:

$$g_i = \int_a^b k_i(x) \cdot f(x) dx \tag{11}$$

It relates measurement data g_i to the inaccessible profile $f(x)$ through the proper weighting function $k_i(x)$ (or kernel, as stated in mathematical terms) distributed over the region $[a, b]$ in which we are interested. The different i usually represent different frequencies at which the measurement has been made; and $k_i(x)$ can be some kind of optical transmission functions.

However, in using most indirect sensing techniques the atmospheric measurements show a certain degree of correlation which leads to the question of the benefit in taking more data points. For example, if dependence exists among the measurements that may allow one of the measurements to be written as a linear combination of the others; such

a measurement is said to be predictable. If the value predicted is within some uncertainty envelope which is less than the experimental noise level, it implies that this value can be predicted better than measured (within the experimental accuracy). In this case, it would be redundant to continue the measurement. Therefore, it is worthwhile to investigate the actual "information content" of such a measurement.

As given by the relationship shown in eq. (11), the dependence of measurements usually comes from the physical properties of the kernels, which may not all be linearly independent for all $f(x)$. In this case, investigating the degree of independence among kernels will correspond to finding the independence of the measurements, thus to determine the extent of the information contained. There are two advantages of looking into the independence of the kernels. First, in view of the cost of adding and analyzing more data points, determining the independence of kernels (and thus the usefulness of those added measurements) can be done before the measurements have been taken. The same process which provides information content can also assist one in locating from which channels the information comes, thus avoiding redundant measurements. Secondly, in view of resolution, the closer the relationships among the kernels, the more difficult will be the inversion of the profile of $f(x)$. To make this point clear: note that the integral in eq. (11) can be approximated in numerical quadratic summation form, thus can be written in matrix form as $G = KF$, for a finite set of data points and finite measurement intervals. Highly dependent kernels will make the determinant of the kernel matrix very small. Therefore, when one wishes to invert the matrix K in order to find the unknown profile F as in $K^{-1}G = F$, the error (including the truncation error of the computer) will be magnified so much that the information can no longer be obtained. Under such circumstances, special constrained techniques may be considered.

The theory of information content of an experiment is solely based on the presence of noise in the experiment and the nature of the kernels. In principle, one is looking for a set of a 's, which are not all zero simultaneously, such that $\sum_{i=1}^N a_i k_i(x) = 0$. Then one of the kernels can be written as a linear combination of the others, thus it is predictable.

However, the above summation may not vanish in the general case because there exists some uncertainty, both experimentally and in the numerical approximations adopted. Hence instead, we search for the set of a 's that minimizes $\sum_{i=1}^N a_i k_i(x)$ and subjects them to a chosen constraint, say $\sum_{i=1}^N a_i^2 = 1$. (The absolute magnitudes of the a 's are irrelevant.) As long as the summation is less than or equal to the noise level for all x in $[a, b]$, one kernel can be predicted within the experimental accuracy.

Thus the information provided by this kernel will be lost in the noise, and the number of independent pieces of information must be reduced by one. An appropriate method to minimize such a quantity (which is a function of x) is to look for the minimum values of its quadratic form

$q = \int \left| \sum_{i=1}^N a_i k_i(x) \right|^2 dx$, this can be written in vector notation as:

$$q = \int [a^* k(x)] [k^*(x) a] dx = a^* \left[\int k(x) k^*(x) dx \right] a = a^* C a \quad (12)$$

where a is not a function of x , and $a, k(x)$ are column vectors. C is the covariance matrix of k , $C = \left[\int k(x) k^*(x) dx \right]$. Applying the eigenvalue theorem (Courant and Hilbert, 1953) subject to the constraint that

$\sum_{i=1}^N a_i^2 = 1$, the extremum values of q are given by λ_i , the eigenvalues of the covariance matrix C , if a is chosen to be the corresponding

normalized eigenvectors U_i . Thus $C = U \Lambda U^*$ and $q = a^* C a = U_i^* U \Lambda U_i^* = \lambda_i$

where U, Λ are eigenvector and eigenvalue matrix, respectfully. Therefore,

the smallest eigenvalue λ_m provides the minimum value of q and the magnitude

of $\sum_{i=1}^N a_i k_i(x)$ for all x in $[a, b]$ is $\sqrt{\lambda}$. (Since the covariance matrix C is a positive definite symmetric matrix, the corresponding eigenvalues are all positive and non zero.) If one of the eigenvalues, λ , is smaller than the estimated measurement plus computational error, the number of independent kernels or information content should be decreased by one. If p of the eigenvalues are smaller than the noise level, the number should be decreased by p .

The above statement can be shown clearly though the effect of $k_i(x)$ in g_i . Now consider the error ϵ_i contained in the measurement g_i as given in eq. (11)

$$g_i + \epsilon_i = \int_a^b k_i(x) f(x) dx \quad (13)$$

Assuming k_ℓ is predictable, then the corresponding prediction of g_ℓ can be written as a linear combination of the other measurement values g_i , as in g_ℓ (pred.) = $\frac{-1}{a_\ell} \sum_{i=1, i \neq \ell}^N (a_i g_i)$. The measurement value g_ℓ can be calculated by multiplying eq. (13) through by a_i , summing all the i 's, and readjusted the terms, we get:

$$g_\ell + \left[\frac{1}{a_\ell} \sum_{i=1}^N a_i \epsilon_i \right] = \frac{-1}{a_\ell} \sum_{i=1, i \neq \ell}^N a_i g_i + \left\{ \frac{1}{a_\ell} \int_a^b \left[\sum_{i=1, i \neq \ell}^N a_i k_i(x) \right] f(x) dx \right\} \quad (14)$$

Apparently the first term on the right hand side of eq. (14) is g_ℓ (pred.) (an estimate of g_ℓ). In this case, one can estimate g_ℓ closer than one can measure it, if the second term on the right hand side of the eq. (14) is less than or equal to the error term (the second term) on the left hand side of the equation, i.e. if

$$\left| \int_a^b \left[\sum_{i=1, i \neq \ell}^N a_i k_i(x) \right] \cdot f(x) dx \right| \leq \left| \sum_{i=1}^N a_i \epsilon_i \right| \quad (15)$$

Applying the Schwarz's inequality and the mean value theorem on the left hand side of the inequality, eq. (15) we find that:

$$\left| \int_a^b \sum_{i=1}^N a_i k_i(x) \cdot f(x) dx \right|^2 \leq \left| \int_a^b \sum_{i=1}^N a_i k_i(x) dx \right|^2 \cdot |f_m(x)|^2$$

The minimized quantity, $\left| \int_a^b \sum_{i=1}^N a_i k_i(x) dx \right|^2$ is the smallest eigenvalue λ_m of the covariance matrix C multiplied by a constant which is determined by the integral limits. Thus, if $|f_m(x)|^2$ has order of magnitude one, and with a properly adjusted integral scale $[0,1]$, the upper bound of this quantity would be λ_m .

Again, applying the Schwarz's inequality on the right hand side of eq. (15) above:

$$\left| \sum_i a_i \epsilon_i \right|^2 \leq \left| \sum_i a_i^2 \right| \cdot \left| \sum_i \epsilon_i^2 \right|$$

for an independent randomly distributed error ϵ_i , $\left| \sum_{i=1}^N \epsilon_i^2 \right| = N |\epsilon_{rms}|^2$.

Generally speaking, for a relative error ϵ_i , $\left| \sum_i \epsilon_i^2 \right| = |\epsilon_v|^2$. Hence, it is clear that if λ_m is "less than" $|\epsilon_v|^2$ (or it should be said "much less than", for there is considerable uncertainty when they are the same order of magnitude), the noise to signal ratio is large enough that information cannot be obtained.

Now it is more interesting to know exactly which one or ones of the kernels is predictable: Surely the best approximation can be made by choosing the weakest response kernel. That is, for a given very small eigenvalue λ_m , the correspondent linear combination of kernels can be

approximated to zero. Therefore, the kernel k_j , whose coefficient has the largest value, can be thought of as the most weakly represented base function. Therefore, the corresponding normalized kernel, k_j , should be the least useful.

To make the case simple, and to have a direct measure for λ , proper scaling for g , k , and f is necessary and does not change the relationship between them. On the other hand, it provides a convenient way to estimate the relative error. As pointed out earlier, g_i can be scaled having an order of one, then the ϵ_i are the relative errors and $|g| \sim N$ (the number of channels). Scaling can also be done such that $|f|^2 \sim 1$ and the kernels are normalized. Then eq. (13) can be written as:

$$\frac{g_i}{\alpha} + \frac{\epsilon_i}{\alpha} = \left(\frac{\beta}{\alpha}\right) \int_a^b k_i(x) \cdot \left[\frac{1}{\beta} \cdot f(x)\right] dx \quad (16)$$

Where α , β are proper scaling factors.

Also, the integral limits can be rescaled from 0 to 1. Without proper scaling there can be confusion between the comparison of eigenvalues and the noise levels, which has been pointed out by Twomey (1974) in his earlier papers.

Such eigenvalue techniques can also be used to directly analyze the unknown function, $f(x)$, by introducing a new set of orthonormal functions $\phi(x)$ on which $f(x)$ can be projected, then $f(x) = \sum_j \xi_j \phi_j(x)$. However, such a new orthonormal set of $\phi_j(x)$ must satisfy eq. (11) and should be constrained to $k_i(x)$. Therefore in general, $\phi_j(x)$ is chosen as a linear combination of all the kernels, and the normalization constraint will determine the correspondent coefficients. It turns out that the best choice of $\phi_j(x)$ is $\frac{1}{\lambda_j - 1} \sum_{i=1}^N U_{ij} k_i$, where U_{ij} is the i th element of the eigenvector U_j associated with eigenvalue λ_j of the covariance matrix C . Written in matrix form

it will become $\phi_{\lambda}(x) \approx U \Lambda^{-1/2} \cdot k_{\lambda}(x)$. With this substitution in the equation (11), one obtains:

$$\xi_{\lambda} = \Lambda^{-1/2} \cdot U^* \cdot g_{\lambda} \quad (17)$$

and $f(x)$ becomes:

$$f(x) = k_{\lambda}^*(x) \cdot U \cdot \Lambda^{-1} \cdot U^* \cdot g_{\lambda} \quad (18)$$

Obviously, small eigenvalues involved in such an inversion for $f(x)$ will make it very unstable. But it provides a straightforward way to investigate the error magnification which is also a criterion in determining the information content through deleting the measurements which have an excessive error magnification. (Detailed descriptions can be referred in Twomey (1977.)

Although we were concentrating on analyzing the information content of the kernels here, the same method can be applied directly to the measurement data, which has been done in many cases (e.g. Mateer, 1965). If there is one eigenvalue which is less than $|\epsilon_{\lambda}|^2$, one measurement can be predicted better than measured and the information content should be reduced by one. If there are p eigenvalues which are less than $|\epsilon_{\lambda}|^2$, there should be p redundant measurements. For a total of N measurements, the number of pieces of independent information will become $(N-p)$.

4. Results and Discussion

The previous analysis has been applied to investigate the information content of the spectral output of a microwave radiometer used to detect the H_2O content in the stratosphere and mesosphere. This spectral output totals 49 channels, each separated by 50 KHz, ranging from 22.2362798 GHz to 22.2338798 GHz, and centered at 22.2350798 GHz. Since symmetry exists about the center frequency, the information content analysis need only to be done for 25 channels. The altitude range was chosen from 50 Km

to 86 Km., which represents thirty-six, 1 Km layers.

Let us first consider the emission experiment case. The 25 kernels, which have been normalized to unit area for convenience (Fig. 1), were used to do the eigenvalue and eigenvector analysis of their covariance matrix C . The resulting eigenvalues, as listed in Table 1 (only for the ones whose magnitudes are greater than 10^{-9}), show that for a given 1% relative r.m.s. error, four independent pieces of information could safely be drawn, however the fifth may be possible as well. The rapidly decreasing magnitude of the eigenvalues indicates that improving experimental accuracy doesn't provide much more, if any, new information. In this case, many of the 25 measurements will be redundant.

The kernels which contribute the most informations are k_1 , k_{13} , k_{22} , k_{25} , and to a lesser extent k_{24} , where the subscripts represent the corresponding frequencies: 22.2338798, 22.344798, 22.2349298, 22.2350798 and 22.2350298 GHz, respectively (Table II). Their relationship with height have been plotted in Fig. 2. Since the original kernel functions are reasonably smooth and very much overlapped (as shown in Fig. 1), it would not be surprising that they have such limited independence. This means the measurement can be done as well based on these four (or five) channels as with all the original 25 channels to within an experimental uncertainty of about 1%. To make this point more explicitly, the same eigenvalue analysis was applied to an arbitrary set of ten channels; specifically channel numbers 2, 5, 8, 11, 14, 17, 20, 23, 24 and 25 were chosen. The results are also listed in Table I. For the same noise level, apparently four pieces of information is derivable. Under such circumstances, it is obvious that making more measurements does not improve, by much, knowledge concerning the inaccessible profile f .

In Figure 3 we show that the number of independent pieces of information which can be derived for various experimental error levels. If the error lies beyond 5%, there will be only two pieces of information that could be inferred from such 25 measurements. Therefore, even though the discussion of error levels cannot be precise, the number of independent pieces of information is still quite apparent as long as the signal to noise ratio is much greater than 1. Therefore, increasing the number of measurements or improving measurement accuracy may not increase the information content considerably.

5. Zenith Angle Effects

The discussion above was based upon calculations for zero zenith angle operation. In order to increase the signal to noise ratio, the radiometer should be operated at lower elevation angles (i.e. to obtain a longer slant optical path). Therefore, the same analysis has also been applied to the case of the same 25 channels, but with a 70° zenith angle. The resulting eigenvalues were extremely close to the first case, thus for the same relative error it should provide the same number of independent pieces of information. However, the channels which contribute the most information do tend to be redistributed slightly toward the center frequency channel. Since the discussion of information content is based on the competition between the relative error level and the eigenvalues of the measurement kernels, one can only expect that lowering the elevation angle will reduce the noise to signal ratio and may provide one or more additional pieces of information.

The same 70° zenith angle dependence for the absorption case has been done, and the previous argument still holds.

6. Summary and Conclusion

The information content of a microwave radiometer experiment has been investigated. Since the kernel (or weighting) functions are reasonably smooth and very much overlapped, the number of independent pieces of information is much less than the total number of possible measurement channels. This means that if one tries to use all the channels in performing the observation, many of the measurements would be redundant. As for how many independent pieces information can be drawn, this depends on the relative error of the whole experiment which can be reduced by lowering the operating elevation angle or improving the instrument itself. One may argue that taking more data points certainly has some value, but such improvements may not be significant enough to provide additional information; in addition the cost of taking and processing more measurements may be too high. Also, the difficulties of the actual inversion process are magnified by highly dependent kernels, thus it is worthwhile to examine the information content and use such results as a guide.

For the current Penn State system four, or perhaps five, independent pieces of information are attainable with maintenance of reasonably system accuracy.

Table I
(Eigenvalues λ and Corresponding Channel/Kernel Numbers k)

Order of λ	for 10 measurements		for 25 measurements	
	λ	k	λ	k
1	2.99×10^{-1}	(k_{25})	8.40×10^{-1}	(k_{25})
2	9.81×10^{-2}	(k_2)	1.33×10^{-1}	(k_1)
3	1.73×10^{-2}	(k_{23})	3.66×10^{-2}	(k_{22})
4	3.17×10^{-3}	(k_{17})	5.69×10^{-3}	(k_{13})
5	3.47×10^{-4}	(k_{24})	7.93×10^{-4}	(k_{24})
6	5.64×10^{-5}	(k_{20})	1.11×10^{-4}	(k_{18})
7	5.34×10^{-6}	(k_5)	1.37×10^{-5}	(k_{23})
8	1.48×10^{-7}	(k_{14})	1.34×10^{-6}	(k_3)
9	2.02×10^{-9}	(k_{11})	1.06×10^{-7}	(k_{21})
10	*		6.78×10^{-9}	(k_{10})

*Eigenvalues not included in this Table have magnitude much less than 10^{-9} .

Table II (Channel/Kernel Frequency)

Channel/Kernel Number	Frequency (GHz)	Frequency Offset (MHz)
k ₁	22.2338798	1.20
k ₂	22.2339298	1.15
k ₃	22.2339798	1.10
k ₄	22.2340298	1.05
k ₅	22.2340798	1.00
k ₆	22.2341298	0.95
k ₇	22.2341798	0.90
k ₈	22.2342298	0.85
k ₉	22.2342798	0.80
k ₁₀	22.2343298	0.75
k ₁₁	22.2343798	0.70
k ₁₂	22.2344298	0.65
k ₁₃	22.2344798	0.60
k ₁₄	22.2345298	0.55
k ₁₅	22.2345798	0.50
k ₁₆	22.2346298	0.45
k ₁₇	22.2346798	0.40
k ₁₈	22.2347298	0.35
k ₁₉	22.2347798	0.30
k ₂₀	22.2348298	0.25
k ₂₁	22.2348798	0.20
k ₂₂	22.2349298	0.15
k ₂₃	22.2349798	0.10
k ₂₄	22.2350298	0.05
k ₂₅	22.2350798	0.00

Table II (Channel/Kernel Frequency)

Channel/Kernel Number	Frequency (GHz)	Frequency Offset (MHz)
k ₁	22.2338798	1.20
k ₂	22.2339298	1.15
k ₃	22.2339798	1.10
k ₄	22.2340298	1.05
k ₅	22.2340798	1.00
k ₆	22.2341298	0.95
k ₇	22.2341798	0.90
k ₈	22.2342298	0.85
k ₉	22.2342798	0.80
k ₁₀	22.2343298	0.75
k ₁₁	22.2343798	0.70
k ₁₂	22.2344298	0.65
k ₁₃	22.2344798	0.60
k ₁₄	22.2345298	0.55
k ₁₅	22.2345798	0.50
k ₁₆	22.2346298	0.45
k ₁₇	22.2346798	0.40
k ₁₈	22.2347298	0.35
k ₁₉	22.2347798	0.30
k ₂₀	22.2348298	0.25
k ₂₁	22.2348798	0.20
k ₂₂	22.2349298	0.15
k ₂₃	22.2349798	0.10
k ₂₄	22.2350298	0.05
k ₂₅	22.2350798	0.00

References

- Courant, R. and Hilbert, D., 1953: Methods of Mathematical Physics, I. Interscience Publishers, New York, New York.
- Goody, R. M., 1964: Atmospheric Radiation: Theoretical Basis. Clarendon Press, Oxford.
- Longbothum, R. L., 1976: A Study of Water Vapor Measurement in the Stratosphere and Mesosphere Using Microwave Techniques. PSU-IRL-SCI-449, Scientific Report, Ionosphere Research Laboratory, The Pennsylvania State University.
- Mateer, C. L., 1965: On the Information Content of Umkehr Observation, J. Atmos. Sci., 22, pp. 370-381.
- Twomey, S., 1974: Information Content in Remote Sensing, Appl. Opt., 13, pp. 942-945.
- Twomey, S., 1977: Introduction to the Mathematics of Inversion in Remote Sensing and Indirect Measurement. Elsevier Scientific Publishing Company, Amsterdam.

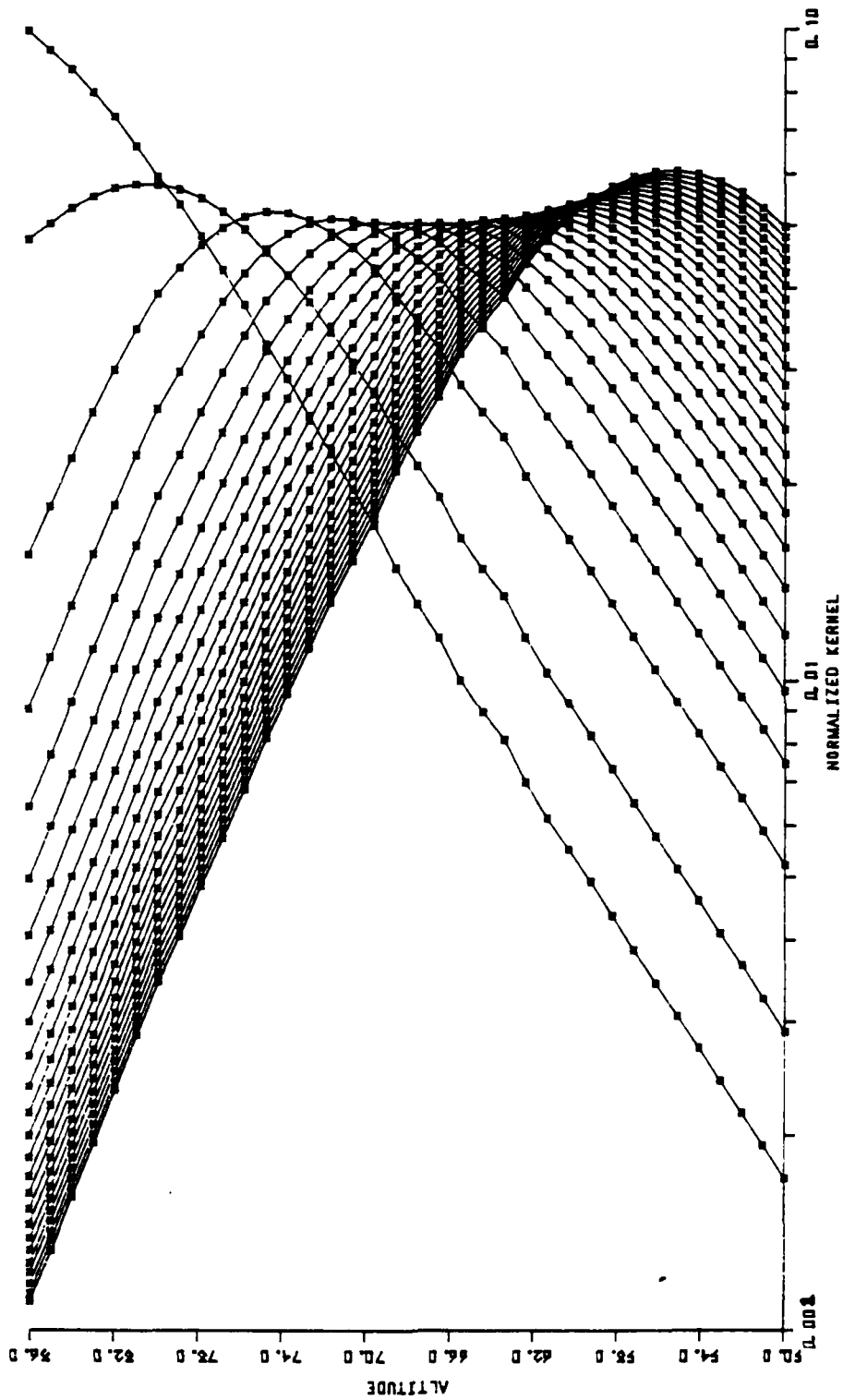


Fig. 1: The 25 normalized kernels plotted against height, zero zenith angle, emission case.

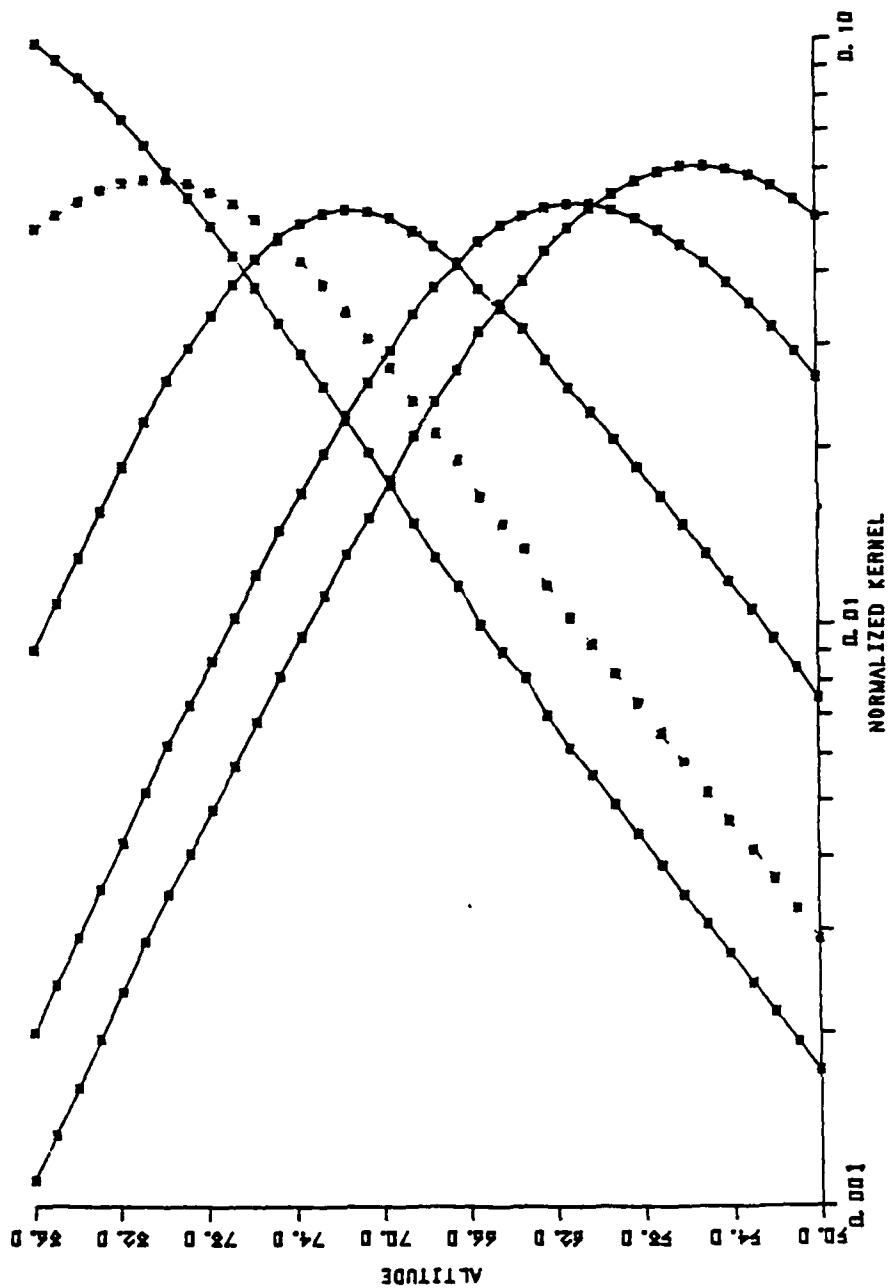


Fig. 2: The four independent (information containing) kernels plotted versus height (solid curves); a possible fifth, information containing, kernel (unconnected symbols).

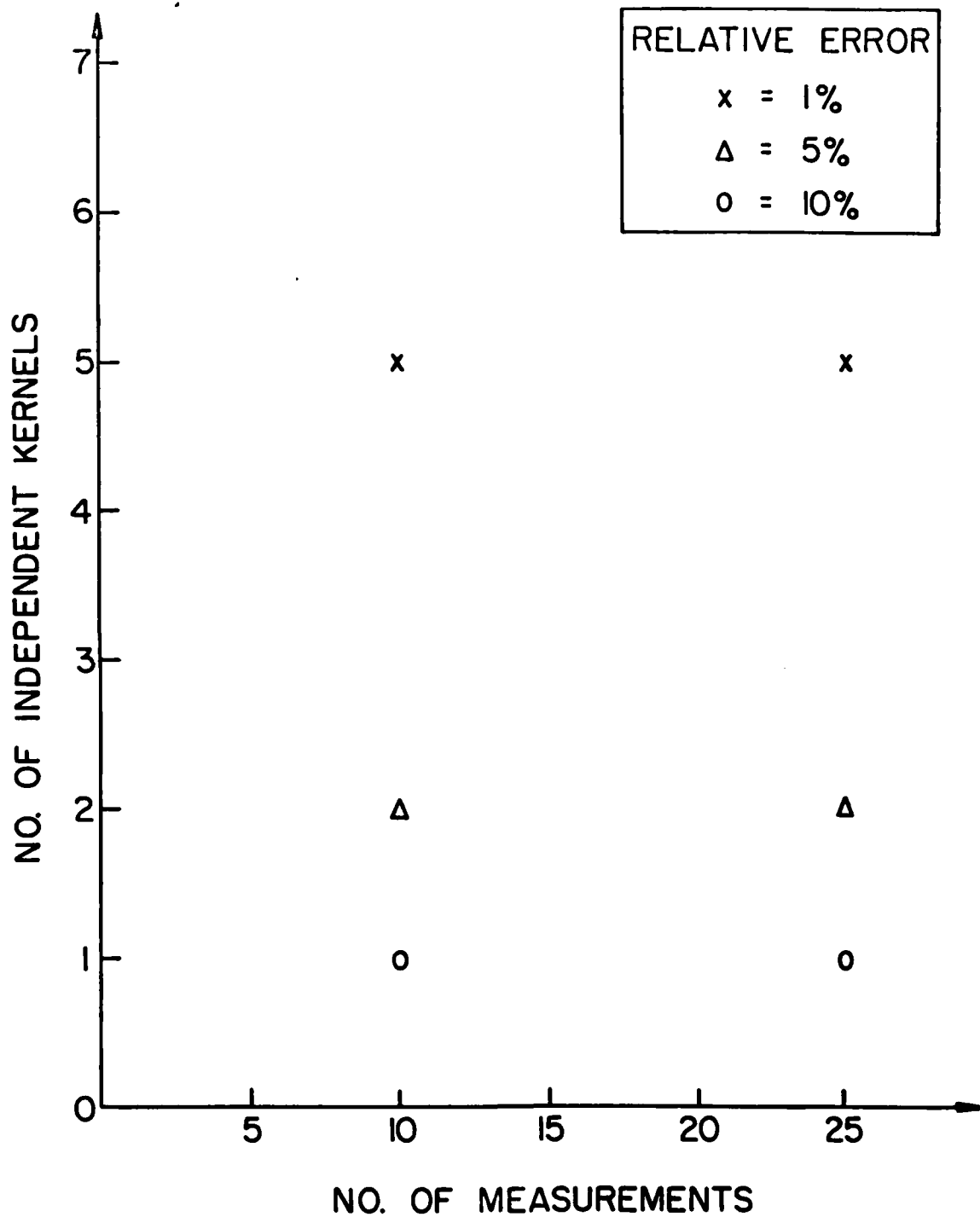


Fig. 3: The estimated number of independent kernels, dependant upon the number of measurements, for different possible error levels.

DISTRIBUTION LIST FOR PENNSYLVANIA STATE
UNIVERSITY REPORTS UNDER ONR CONTRACT
NO. N00014-79-C-0610

Dr. Gene W. Adams
NOAA Lab. R43
Boulder, CO 80302

Dr. A. C. Aiken
Code 625 NASA
Goddard Space Flight Center
Greenbelt, MD 20771

Mr. R. V. Anderson
Naval Research Lab
Code 4320
Washington, DC 20375

Arecibo Observatory
P.O. Box 995
Arecibo, PR 00612
ATTN: Director and Librarian

Dr. E. Arijs
Belgian Inst. for Space Aeronomy
3 Ringlaan
B-1180 Brussels, BELGIUM

Dr. F. Arnold
Max Planck Institut
Fur Kernphysik
Postfach 103980
D169 Heidelberg
GERMANY

Dr. E. Boeck
Professor of Physics
Niagara University
New York NY 14109

Dr. W-M Boerner
COM LAB/INF ENG
UICC
P.O. Box 4348
Chicago, IL 60680

Prof. H. G. Booker
Dept. of Applied Electrophysics
P.O. Box 109
University of California
La Jolla, CA 92038

Dr. S. A. Bowhill
Aeronomy Laboratory
Dept. of Elec. Engineering
363 E. E. Building
University of Illinois
Urbana, IL 61801

Dr. R. R. Burke
CRPE
CRNS
45045 Orleans CEDEX
FRANCE

Dr. J. M. Calo
Dept. of Chem. Eng.
Engineering Quad
Princeton University
Princeton, NJ 08544

Dr. H. R. Carlon
DRDAR-CLB-PO
Chemical Systems Lab
Aberdeen Proving Ground
MD 21010

Prof. A. W. Castleman
Dept. of Chemistry
University of Colorado
Campus Box 215
Boulder, CO 80309

Dr. W. C. Chamedies
School of Geophysical Sciences
Georgia Institute of Technology
Atlanta, GA 30332

DISTRIBUTION LIST FOR PENNSYLVANIA STATE
UNIVERSITY REPORTS UNDER ONR CONTRACT
NO. N00014-79-C-0610

PAGE 2

Comissao Nacional de
Atividades Espaciais
Calisca Postal, 515
San Jose Dos Campos
Sao Paulo, BRAZIL

Director
U.S. Naval Research Lab
Washington, DC 20390
ATTN: Technical Information
Division

Commander and Director
Atmospheric Sciences Lab.
U.S. Army Electronics Commission
DRSEL-BY-SY-A
Dr. Franklin E. Niles
White Sands Missile Range,
NM 88002

Director
U.S. Naval Research Lab
Washington, DC 20390
ATTN: Library, Code 2029

Dr. Cullen Crain
Rand Corporation
1700 Main Street
Santa Monica, CA 90406

Dr. J. C. Dodge
CODE EBT-8
Severe Storms Program Manager
NASA Headquarters
Washington, DC 20546

Dr. D. L. Croom
Rutherford and Appleton
Laboratories
Ditton Park
Slough SL3 9JX
Bucks, ENGLAND

Dr. Bruce Edgar
Box 92957
Aerospace Corp.
Los Angeles, CA 90009

Dr. G. A. Dawson
Inst. of Atmos. Phys.
University of Arizona
Tuscon, AZ 85721

Dr. J. V. Evans
P.O. Box 73
Lexington, MA 02173

Dr. Adarsh Deepak
Institute for Atmospheric
Optics and Remote Sensing
P.O. Box P
Hampton, VA 23666

Dr. A. A. Few
Department of Space Physics
Rice University
P.O. Box 1892
Houston, TX 77001

Defense Technical
Information Center
Building 5
Cameron Station
Alexandria, VA 22314

Dr. W. A. Flood
P.O. Box 5275
Dept. of Elec. Eng.
North Carolina State University
Raleigh, NC 27607

Prof. George Freier
School of Physics and Astronomy
University of Minnesota
Minneapolis, MN 55455

DISTRIBUTION LIST FOR PENNSYLVANIA STATE
UNIVERSITY REPORTS UNDER ONR CONTRACT
NO. N00014-79-C-0610

PAGE 3

Dr. Richard Goldberg
Code 912
Goddard Space Flight Center
Greenbelt, MD 20771

Dr. F. S. Johnson
National Science Foundation
1800 G. Street, N.W.
Washington, DC 20550

Prof. J. Hallett
Atmospheric Science Lab
Stead Facility
Desert Research Institute
Reno, NV 60220

Dr. K. H. Kaselau
Institut Fur Geophysik & Meteo.
Albertus-Magnus-Platz
D5000 Koln 41
WEST GERMANY

Dr. Ake Hedberg
Uppsala Ionospheric Observatory
755 90 Uppsala 1
SWEDEN

Dr. H. Kasemir
1604 S. County Road 15 Rt. 1
Berthoud, CO 80513

Dr. J. R. Herman
624 Tulane Avenue
Melbourne, FL 32901

Dr. Thomas Keneshea
AFGL
L.G. Hanscom Field
Bedford, MA 01730

Dr. F. H. Hibberd
Department of Physics
University of New England
Armidale, N.S.W. 2351
AUSTRALIA

Dr. G. Kockarts
Institut D'Aeronomie Spatiale
Avenue Circulaire 3
B-1180, Bruxelles, BELGIUM

Dr. W. A. Hoppel
CODE 4326
Naval Research Lab
Washington, DC 20375

Dr. W. R. Kuhn
Dept. of Atmospheric
and Oceanic Science
University of Michigan
Ann Arbor, MI 48104

Dr. R. E. Houston
Dept. of Physics
University of New Hampshire
Durham, NH 03824

Dr. D. R. Lane-Smith
60 Cedarwood Crescent
Nobleton, Ontario
LOG 1NO CANADA

Dr. S. G. Jennings
Physics Department
UMIST
Sackville Street
Manchester M60 1QD
ENGLAND

Dr. L. J. Lanzerotti
Bell Laboratories
Murray Hill, NJ 07974

DISTRIBUTION LIST FOR PENNSYLVANIA STATE
UNIVERSITY REPORTS UNDER ONR CONTRACT
NO. N00014-79-C-0610

PAGE 4

Prof. J. Latham
Physics Department
Sackville Street
Manchester M60 1QD
ENGLAND

Library
Service D'Aeronomie
CNRS
91 Verreries - Le Buisson
Paris, FRANCE

Dr. Joseph Lemaire
Institut D'Aeronomie Spatiale
Avenue Circulaire 3
B-1180 Bruxelles, BELGIUM

Dr. R. Markson
46 Kendal Common Road
Weston, MA 02193

Prof. Z. Levin
Dept. of Geophysics
& Planetary Sciences
Tel Aviv University
Tel Aviv, ISRAEL

Massachusetts Institute
of Technology
Center for Space Research
Reading Room, Rm. 37-582
Cambridge, MA 02139

Dr. Lhermitte
School of Marine &
Atmospheric Science
University of Miami
Miami, FL 33124

Mr. M. T. McCracken
Resident Representative
Department of the Navy
Carnegie Mellon University
Room 407 Margaret Morrison Bldg.
Pittsburgh, PA 15213

Library
Department of Meteorology
University of Stockholm
Arrhenius Laboratory
Fack S-104 05 Stockholm
SWEDEN

Prof. E. W. McDaniel
School of Physics
Georgia Inst. of Technology
Atlanta, GA 30332

Library
Geophysical Institute
University of Alaska
College, AK 99701

Dr. L. R. Megill
Director, Center for
Atmospheric and Space Sciences
Logan State University
Logan, UT 84321

Library
Max-Planck-Institut
Für Aeronomie
3411 Lindau/Harz
Gillersheim, WEST GERMANY

Dr. R. E. Meyerott
27100 Elena Road
Los Altos Hills, CA 94022

Dr. A. P. Mitra
Head, Center of
Radiophysics and Aeronomy
National Physical Laboratory
New Delhi-12, INDIA

DISTRIBUTION LIST FOR PENNSYLVANIA STATE
UNIVERSITY REPORTS UNDER ONR CONTRACT
NO. N00014-79-C-0610

PAGE 5

Dr. V. A. Mohnen
State University of
New York at Albany
1400 Washington Avenue
Albany, NY 12222

Dr. C. B. Moore
Physcis Department
NMIMT
Socorro, NM 87801

Prof. R. Muhleisen
Astronomisches Institut
De Universitat Tubingen
Aussenstelle Weissenau
798 Drasthalde/Ravensburg
WEST GERMANY

Dr. A. F. Nagy
Space Physics Research Lab.
Dept. of Elec. Engineering
University of Michigan
2455 Hayward, North Campus
Ann Arbor, MI 48105

Dr. Rocco S. Narcissi
AFGL
L.G. Hanscom Field
Bedford, MA 01730

Dr. Marcel Nicolet
30 Avenue Den Doorn
B-1180 Brussels
BELGIUM

Dr. R. O. Olsen
Atmospheric Sciences Laboratory
White Sands Missile Range,
NM 88002

Dr. D. E. Olson
Department of Physics
University of Minnesota, Duluth
Duluth, MN 55812

Dr. R. E. Orville
SUNY
Albany, NY 12222

Dr. Chung Park
Radioscience Laboratory
Stanford Electronics Laboratories
Stanford University
Stanford, CA 94305

Dr. L. W. Parker
252 Lexington Road
Concord, MA 01742

Dr. Hays Penfield
Harvard University
Cambridge, MA 02139

Dr. J. Podzimek
University of Missouri-Rolla
Cloud Physics
Rolla, MO 65401

Dr. George C. Reid
NOAA R44
Boulder, CO 80302

Dr. R. Reiter
Inst. F. Atmosph.
Umwelt Forschung
Kreuzeckbahnstrasse 19
D-8100 Garmisch-Partenkirchen
WEST GERMANY

Dr. James Rosen
University of Wyoming
Department of Physics
and Astronomy
Laramie, WY 82071

Dr. L. H. Ruhnke
Naval Research Laboratory
Code 4320
Washington, DC 20375

DISTRIBUTION LIST FOR PENNSYLVANIA STATE
UNIVERSITY REPORTS UNDER ONR CONTRACT
NO. N00014-79-C-0610

PAGE 6

Prof. O. E. H. Rydbeck
Onsala Space Observatory
Research Laboratory
of Electronics
Chalmers University of Technology
Onsala, SWEDEN

Dr. F. J. Schmidlin
NASA
Wallops Flight Center
Wallops Island, VA 23367

Dr. P. R. Schwartz
E. O. Hulbert Center
for Space Research
Naval Research Laboratory
Washington, DC 20375

Dr. Ron Schwiesow
NOAA ERL WPL
Boulder, CO 80302

Dr. C. F. Sechrist
University of Illinois
Electrical Engineering Dept.
Urbana, IL 61801

Official Publications Section
British Library Reference Division
London, WC1B 33DG
ENGLAND

Dr. T. A. Seliga
Director
The Atmospheric Sciences Program
Ohio State University
Columbus, OH 43210

Space Science Board
Documents Section
(JH No. 421)
National Academy of Sciences
2101 Constitution Avenue, N.W.
Washington, DC 20037

Dr. P. Stubbe
Max-Planck-Institut Fur Aeronomie
3411 Lindau-Harz
Gillersheim, GERMANY

Dr. Paul Swanson
Jet Propulsion Laboratory
4800 Oak Grove Drive
Pasadena, CA 91103

Dr. Wesley E. Swartz
School of Electrical Engineering
Phillips Hall
Cornell University
Ithaca, NY 14850

Dr. W. A. Swider
AFGL (LKB)
L.G. Hanscom Field
Bedford, MA 01730

Technical Reports Collection
Gordon McKay Library
Harvard University
Pierce Hall, Oxford Street
Cambridge, MA 01020

Dr. D. L. Thacker
E. O. Hulbert Center
for Space Research
Naval Research Laboratory
Washington, DC 20375

Dr. E. V. Thrane
NDRE, P.O. Box 25
N-2007 Kjeller
NORWAY

Dr. B. A. Thrush
Dept. of Physical Chemistry
Lensfield Road
Cambridge, ENGLAND

DISTRIBUTION LIST FOR PENNSYLVANIA STATE
UNIVERSITY REPORTS UNDER ONR CONTRACT
NO. N00014-79-C-0610

PAGE 7

Dr. Thomas F. Trost
Electrical Engineering Dept.
Texas Tech. University
Lubbock, TX 79409

Dr. Roland T. Tsunoda
Radio Physics Laboratory
Stanford Research Institute
333 Ravenswood Avenue
Menlo Park, CA 94025

Dr. R. P. Turko
R&D Associates
P.O. Box 9695
Marina Del Rey, CA 90291

Dr. J. W. Waters
Jet Propulsion Laboratory
4800 Oak Grove Drive
Pasadena, CA 91103

Dr. S. Weisbrod
Mgr. Electromagnetic
Propagation Department
Micronetics
7155 Mission Gorge Road
P.O. Box 20396
San Diego, CA 92120

Dr. J. C. Willett
Code 4325
Naval Research Lab
Washington, DC 20375

World Data Centre
Appleton Lab, Ditton Park
Slough SL3 9JX
Bucks, ENGLAND

<u>Addressee</u>	<u>No. of Copies</u>
Director Defense Nuclear Agency Washington, D.C. 20305 Attn: Dr. Carl Fitz (RAAE)	1
Mr. Dow Evelyn (RAAE)	1
Director Defense Advanced Research Projects Agency 1400 Wilson Boulevard Arlington, VA 22209 Attn: STO	1
LCOL G. Bulin (NMRO)	1
Office of Assistant Secretary of the Navy for Research, Engineering and Systems Washington, D.C. 20301 Attn: Dr. Herbert Rabin	1
Deputy Assistant Secretary of Defense (C ³) The Pentagon Washington, D.C. 20301 Attn: Dr. Thomas P. Quinn Room 3E160	1
Chief of Naval Research 800 N. Quincy Street Arlington, VA 22217 Attn: R. G. Joiner (Code 464)	1
J. Hughes (Code 465)	1
W. Martin (Code 465)	1
H. Mullaney (Code 427)	1
C. Luther (Code 461)	1
S. Reed (Code 100C)	1
W. Boyer (Code 200)	1
Director Naval Electronic Systems Command Washington, D.C. 20360 Attn: PME 117-21	2
PME 117-23	2
PME 117T	2
Director Naval Oceans System Center 271 Catalina Blvd. San Diego, CA 92152 Attn: Dr. Juergen Richter	2

Addressee

No. of Copies

Director
Naval Underwater Systems Center
New London Laboratory
New London, CT 06320
Attn: Dr. Peter Banister

2

Lockheed Palo Alto Research Laboratories
3251 Hanover Street
Palo Alto, CA 94304
Attn: Dr. J. B. Reagan
Dr. Wm. Imhof
Dr. Billy McCormick

1

1

1

Tsao, Jung-Jung. Information Content Analysis for the Penn State Upper Atmospheric Water Vapor-Microwave Radiometer Experiment. The Electrical Engineering Department, Ionosphere Research Laboratory, Electrical Engineering East, University Park, Pennsylvania, 16802, 1981.

PSU-IRL-SCI-468
Classification Numbers:

- 1.9 Structure of the Upper Atmosphere
- 3.2.1 Ground-Based Techniques and Measurements
- 3.2.3 Data Analysis Techniques

A ground based, microwave radiometer system is being completed at IRL which will be used to measure mesospheric water vapor. The present study addresses itself to the basic radiative transfer of this experiment and to the interaction between the atmosphere and electromagnetic radiation.

Using a classical mathematical analysis of the data inversion process an estimation of the true information content of the received data is produced. This process depends critically upon the structure of the weighting functions as was anticipated. The result of this study is that the present radiometer system should have four nearly independent pieces of information per profile, with a fifth piece possible, for realistic estimates of system errors.

Tsao, Jung-Jung. Information Content Analysis for the Penn State Upper Atmospheric Water Vapor-Microwave Radiometer Experiment. The Electrical Engineering Department, Ionosphere Research Laboratory, Electrical Engineering East, University Park, Pennsylvania, 16802, 1981.

PSU-IRL-SCI-468
Classification Numbers:

- 1.9 Structure of the Upper Atmosphere
- 3.2.1 Ground-Based Techniques and Measurements
- 3.2.3 Data Analysis Techniques

A ground based, microwave radiometer system is being completed at IRL which will be used to measure mesospheric water vapor. The present study addresses itself to the basic radiative transfer of this experiment and to the interaction between the atmosphere and electromagnetic radiation.

Using a classical mathematical analysis of the data inversion process an estimation of the true information content of the received data is produced. This process depends critically upon the structure of the weighting functions as was anticipated. The result of this study is that the present radiometer system should have four nearly independent pieces of information per profile, with a fifth piece possible, for realistic estimates of system errors.

Tsao, Jung-Jung. Information Content Analysis for the Penn State Upper Atmospheric Water Vapor-Microwave Radiometer Experiment. The Electrical Engineering Department, Ionosphere Research Laboratory, Electrical Engineering East, University Park, Pennsylvania, 16802, 1981.

PSU-IRL-SCI-468
Classification Numbers:

- 1.9 Structure of the Upper Atmosphere
- 3.2.1 Ground-Based Techniques and Measurements
- 3.2.3 Data Analysis Techniques

A ground based, microwave radiometer system is being completed at IRL which will be used to measure mesospheric water vapor. The present study addresses itself to the basic radiative transfer of this experiment and to the interaction between the atmosphere and electromagnetic radiation.

Using a classical mathematical analysis of the data inversion process an estimation of the true information content of the received data is produced. This process depends critically upon the structure of the weighting functions as was anticipated. The result of this study is that the present radiometer system should have four nearly independent pieces of information per profile, with a fifth piece possible, for realistic estimates of system errors.

Tsao, Jung-Jung. Information Content Analysis for the Penn State Upper Atmospheric Water Vapor-Microwave Radiometer Experiment. The Electrical Engineering Department, Ionosphere Research Laboratory, Electrical Engineering East, University Park, Pennsylvania, 16802, 1981.

PSU-IRL-SCI-468
Classification Numbers:

- 1.9 Structure of the Upper Atmosphere
- 3.2.1 Ground-Based Techniques and Measurements
- 3.2.3 Data Analysis Techniques

A ground based, microwave radiometer system is being completed at IRL which will be used to measure mesospheric water vapor. The present study addresses itself to the basic radiative transfer of this experiment and to the interaction between the atmosphere and electromagnetic radiation.

Using a classical mathematical analysis of the data inversion process an estimation of the true information content of the received data is produced. This process depends critically upon the structure of the weighting functions as was anticipated. The result of this study is that the present radiometer system should have four nearly independent pieces of information per profile, with a fifth piece possible, for realistic estimates of system errors.

DATE
FILMED
-8